

On the parameterization of turbulent surface fluxes over heterogeneous sea ice surfaces

D. Schröder

Meteorological Institute, University of Hamburg, Hamburg, Germany

T. Vihma

Finnish Institute of Marine Research, Helsinki, Finland

A. Kerber and B. Brümmer

Meteorological Institute, University of Hamburg, Hamburg, Germany

Received 12 March 2002; revised 4 February 2003; accepted 3 April 2003; published 19 June 2003.

[1] Turbulent surface fluxes of momentum and sensible and latent heat as well as surface temperature, air temperature, air humidity, and wind speed were measured by the German Falcon research aircraft over the marginal ice zone (MIZ) of the northern Baltic Sea and the Fram Strait. Applying the bulk formulas and the stability functions to the measurements, the roughness lengths for momentum z_0 , sensible heat z_T , and latent heat z_q were calculated. As mean values over a wide range of sea ice conditions, we obtain $z_0 = 5 \times 10^{-4}$ m, $z_T = 1 \times 10^{-8}$ m, and $z_q = 1 \times 10^{-7}$ m. These correspond to the following mean values (\pm standard deviations) of neutral transfer coefficients reduced to 10 m height, $C_{DN10} = (1.9 \pm 0.8) \times 10^{-3}$, $C_{HN10} = (0.9 \pm 0.3) \times 10^{-3}$, and $C_{EN10} = (1.0 \pm 0.2) \times 10^{-3}$. An average ratio of $z_0/z_T \approx 10^4$ was observed over the range of 10^{-6} m $< z_0 < 10^{-2}$ m and differs from previously published results over compact sea ice ($10^{-1} < z_0/z_T < 10^3$). Other observational results over heterogeneous sea ice do not exist. However, our z_0/z_T ratio approximately agrees with observations over heterogeneous land surfaces. Flux parameterizations based on commonly used roughness lengths ratios ($z_0 = z_T = z_q$) overestimate the surface heat fluxes compared to our measurements by more than 100%. **INDEX TERMS:** 3379 Meteorology and Atmospheric Dynamics: Turbulence; 3339 Meteorology and Atmospheric Dynamics: Ocean/atmosphere interactions (0312, 4504); 3307 Meteorology and Atmospheric Dynamics: Boundary layer processes; 3349 Meteorology and Atmospheric Dynamics: Polar meteorology; **KEYWORDS:** turbulent surface fluxes, roughness lengths, marginal ice zone, aircraft measurements

Citation: Schröder, D., T. Vihma, A. Kerber, and B. Brümmer, On the parameterization of turbulent surface fluxes over heterogeneous sea ice surfaces, *J. Geophys. Res.*, 108(C6), 3195, doi:10.1029/2002JC001385, 2003.

1. Introduction

[2] Turbulent surface fluxes are an important link between the atmosphere and the underlying surface (ocean, ice, land). World-wide area-covering flux measurements do not exist, but these fluxes are nevertheless needed in all atmosphere-ocean-ice-land models. Direct flux measurements only exist from special field experiments or at certain places because of the high experimental effort. Results from such limited campaigns are nevertheless applied for general use, simply because there is no other possibility. The application of such results in case of heterogeneous surfaces is particularly questionable. Direct flux measurements over heterogeneous land surfaces are rare, and they are particularly rare over broken, heterogeneous sea ice. Because of the logistic difficulties of surface-based flux measurements

in the latter case, aircraft measurements are the only method to obtain spatially representative results. In this paper, such aircraft measurements are used to derive turbulent flux parameterizations over broken sea ice.

[3] The turbulent surface fluxes of momentum τ , sensible heat H , and latent heat LE are generally parameterized by the bulk formulas,

$$\tau = \rho C_{Dz} V^2, \quad (1)$$

$$H = \rho c_p C_{Hz} (\theta_s - \theta_z) V, \quad (2)$$

$$LE = \rho \gamma C_{Ez} (q_s - q_z) V, \quad (3)$$

where ρ is the density, c_p is the specific heat of air, γ is the latent heat of vaporization, V is the wind speed, and $\theta_s - \theta_z$ and $q_s - q_z$ are the differences in potential temperature and

specific humidity, respectively, between the surface s and a height z in the atmosphere. Applying the Monin-Obukhov similarity theory, the transfer coefficients for momentum C_{Dz} , sensible heat C_{Hz} , and latent heat C_{Ez} , can be determined as functions of the roughness lengths for momentum z_0 , sensible heat z_T , and latent heat z_q , and of the respective universal stability functions ψ_M , ψ_H , and ψ_E [e.g., *Holtsglag and de Bruin*, 1988; *Högström*, 1988],

$$C_{Dz} = \kappa^2 [\ln(z/z_0) - \psi_M(z/L)]^{-2}, \quad (4)$$

$$C_{Hz} = \kappa^2 [\ln(z/z_0) - \psi_M(z/L)]^{-1} \times [\ln(z/z_T) - \psi_H(z/L)]^{-1}, \quad (5)$$

$$C_{Ez} = \kappa^2 [\ln(z/z_0) - \psi_M(z/L)]^{-1} \times [\ln(z/z_q) - \psi_E(z/L)]^{-1}, \quad (6)$$

where κ is the von Karman constant and L is the Obukhov length.

[4] If the turbulent fluxes τ , H , and LE as well as the mean quantities V , θ_s , θ_z , q_s , q_z , and ρ are measured, and if the stability functions are known, the roughness lengths z_0 , z_T , and z_q can be determined from equations (4) and (5) with use of equations (1)–(3) as

$$z_0 = z \left[\exp \left((\rho \kappa^2 V^2 / \tau)^{1/2} + \psi_M(z/L) \right) \right]^{-1}, \quad (7)$$

$$z_T = z \left[\exp \left(\frac{\rho c_p \kappa^2 (\theta_s - \theta_z) V}{H [\ln(z/z_0) - \psi_M(z/L)]} + \psi_H(z/L) \right) \right]^{-1}, \quad (8)$$

$$z_q = z \left[\exp \left(\frac{\rho \gamma \kappa^2 (q_s - q_z) V}{LE [\ln(z/z_0) - \psi_M(z/L)]} + \psi_E(z/L) \right) \right]^{-1}. \quad (9)$$

[5] Over heterogeneous surfaces the turbulent fluxes can be calculated by two different methods: the flux aggregation and the parameter aggregation method. If the flux aggregation method is applied, a separate flux is parameterized for each surface type and the various fluxes are area-averaged thereafter. Applying the parameter aggregation, all quantities (V , θ_s , θ , q) in equations (1)–(3) are averaged over all surface types and applied for the flux parameterization thereafter. In the latter case, the roughness lengths are representative not for the individual surface types but for the integral effect of all surfaces and are called effective roughness lengths (z_0^{eff} , z_T^{eff} , and z_q^{eff}).

[6] Roughness length estimates have been reported in the literature for various surface types. Results for open water, sea ice, and heterogeneous surfaces are summarized in the following.

1.1. Roughness Lengths Over Open Water

[7] Many observations have been made on the roughness length for momentum z_0 over open water. Over a sea surface with mature wind-generated waves far from the coast, z_0 has a well-known dependence on wind speed [*Charnock*, 1955]. Depending on phase of wave development and direction of wave propagation with respect to the wind, z_0 can, however, vary a lot [*Donelan et al.*, 1993]. *DeCosmo et al.* [1996]

found that, in contrast to z_0 , z_T and z_q decrease with increasing wind speed and are 2 to 3 orders of magnitude smaller than z_0 for $V > 15 \text{ m s}^{-1}$.

1.2. Roughness Lengths Over Sea Ice

[8] A review for z_0 over sea ice is given by *Guest and Davidson* [1991]. A widely applied equation relating z_0 to the geometric properties of the surface has been presented by *Banke et al.* [1980]. Over bluff roughness elements, like sea ice with ridges, floe edges, and patterns of snow-drift, z_T depends on z_0 and the roughness Reynolds number $Re = z_0 \times u_\star / \nu$, where u_\star is the friction velocity and ν the kinematic viscosity of air. A theoretical relation for this dependence was derived by *Andreas* [1987]: The ratio z_0/z_T is less than 1 for very smooth ice, about 10^1 for typical sea ice with $z_0 = 1 \text{ mm}$, and increases to 10^3 for $z_0 = 5 \text{ mm}$. The results of *Launiainen et al.* [2001] are approximately comparable to it. Over melting glacier ice in Greenland, a reversed ratio of $z_0/z_T \leq 10^{-2}$ and a high degree of scatter were found by *Calanca* [2001].

1.3. Roughness Lengths Over Heterogeneous Surfaces

[9] *Mai et al.* [1996] have shown that the z_0^{eff} over broken sea ice can exceed the z_0 of compact sea ice because of the form drag due to floe edges and ice ridges, and parameterization schemes have been developed to take this effect into account [e.g., *Uotila*, 2001]. Formulas for z_q^{eff} have been derived for heterogeneous land surfaces [e.g., *Wood and Mason*, 1991], but we are not aware of results particularly derived for broken sea ice. Over heterogeneous surfaces in general, the ratio of the roughness lengths may differ drastically from the ratios which were presented above for homogeneous sea ice and open water. For example, *Beljaars and Holtsglag* [1991] and *Mahrt and Ek* [1993] observed a ratio of $z_0^{eff}/z_T^{eff} = 10^4$ for heterogeneous land surfaces, and *Beljaars and Viterbo* [1994] concluded that using a ratio of 10^3 instead of 10^0 or 10^1 the ECMWF model produces better winter evaporation over land. *Beljaars* [1994] even observed a ratio of 10^7 for a heterogeneous pasture land.

[10] Although observations over various surface types have indicated significant differences between the roughness lengths for momentum, heat, and moisture, this is usually not taken into account in models. For example, *Garratt* [1993] reviewed more than 30 large-scale models, and all of them applied identical roughness lengths for momentum, heat, and moisture.

1.4. Objectives

[11] The objective of this paper is to derive effective roughness lengths z_0^{eff} , z_T^{eff} , and z_q^{eff} and the corresponding neutral transfer coefficients C_{DN10} , C_{HN10} , and C_{EN10} from aircraft observations over broken sea ice. In the following we omit the superscript *eff* for simplicity. Over homogeneous surfaces, the data required for deriving roughness lengths can be gained from measurements at a fixed place, but over heterogeneous surfaces, particularly over broken sea ice, only aircraft measurements are applicable. The results presented here are derived from three field experiments in the marginal ice zones (MIZ) of the northern Baltic Sea (the Baltic Air-Sea-Ice Study (BASIS) [*Launiainen*, 1999] in February/March 1998) and of the Fram Strait (the Arctic Climate System Study (ACSYS) [*Brümmer and Thiemann*, 1999] in

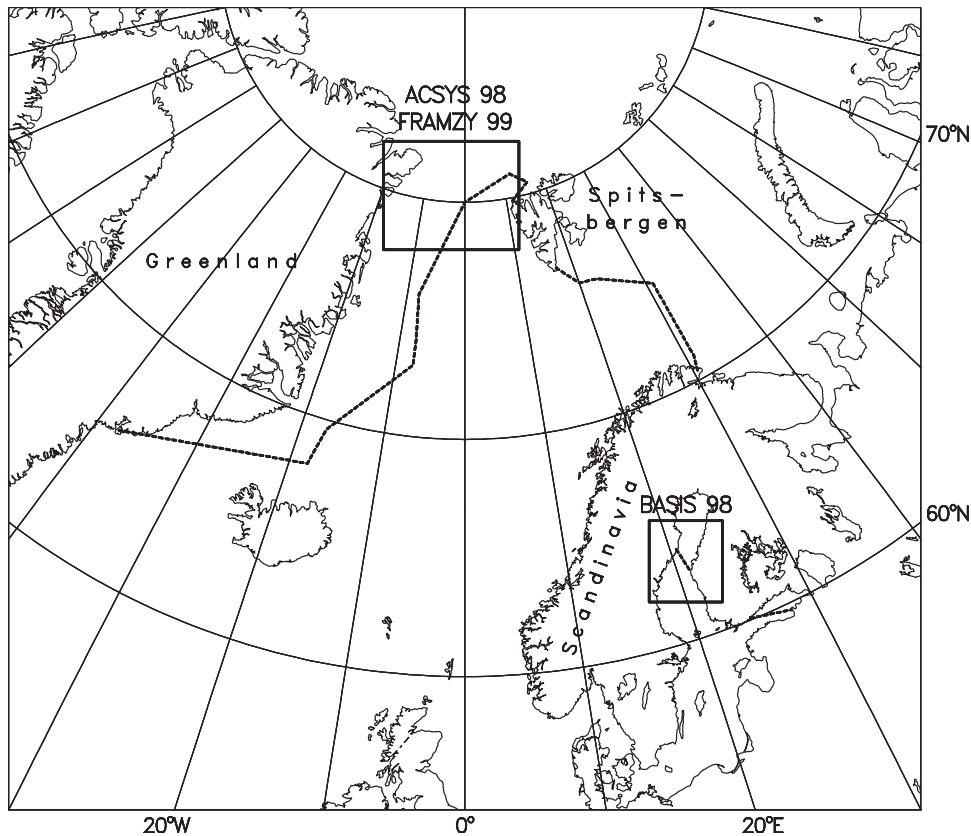


Figure 1. Locations of the three field experiments BASIS, ACSYS, and FRAMZY and the approximate ice edge during March 1998.

March 1998 and the Fram Strait Cyclone Experiment (FRAMZY) [Brümmer, 2000] in April 1999).

[12] The paper is organized as follows. The aircraft observations and the method and accuracy of turbulent flux calculation are presented in section 2. Section 3 deals with the sea ice characteristics during the aircraft flights. The results for the roughness lengths and transfer coefficients and the sensitivity to measurement errors are discussed in section 4. The impact of the new z_0/z_T -ratio on the parameterized heat flux is demonstrated in section 5.

2. Aircraft Observations

2.1. Aircraft Instrumentation and Location of Measurements

[13] The Falcon research aircraft was equipped with a gust-probe system to measure the three wind components. The relative wind was determined by a five-hole wind probe (Rosemount 858J) at a 4-m-long nose boom and the aircraft velocity by an inertial reference system (Honeywell) and GPS. The wind components, air temperature (Pt-100), specific humidity (Lyman- α -humidimeter, Vaisala humicap, and dewpoint mirror) and pressure (pitot tube) were sampled with a frequency of 100 Hz corresponding to a spatial resolution of 1 m at the typical flight speed of 100 m s^{-1} . Furthermore, downward and upward solar as well as long-wave radiation fluxes were measured by pyranometers and pyrgeometers, respectively, and the surface temperature by an infrared radiometer. The latter quantities were sampled with 10 Hz.

[14] The experimental areas of BASIS 1998, ACSYS 1998, and FRAMZY 1999 are presented in Figure 1. A total of 17 missions were flown by the German Falcon research aircraft and took place under a wide range of synoptic situations. During all missions, vertical profiles and horizontal legs were flown in the lowest 3 km. This study utilizes only the horizontal legs flown at low levels between 9 and 35 m to measure the surface fluxes along distances of 20 to 240 km.

2.2. Calculation of Aircraft-Based Turbulent Fluxes

[15] The aircraft-based turbulent fluxes of momentum τ , sensible heat H , and latent heat LE , were calculated according to their definitions as

$$\tau = \rho \times \sqrt{(\overline{w'u'})^2 + (\overline{w'v'})^2}, \quad (10)$$

$$H = \rho \times c_p \times \overline{w'\Theta'}, \quad (11)$$

$$LE = \rho \times \gamma \times \overline{w'q'}, \quad (12)$$

where u , v , and w are the three wind components and $\overline{w'x'}$ is the eddy covariance, where w is the vertical wind and x stands for potential temperature Θ , specific humidity q , or the horizontal wind components u and v . A prime (x') denotes the deviation from the average (\bar{x}). A linear trend was removed before applying the eddy correlation technique. To determine proper sampling lengths for the turbulent

fluxes, calculations were performed varying the sampling length between 1 and 30 km.

[16] A demonstration of the impact of the sampling length and of the horizontal variability of the fluxes is given in Figure 2. The heat fluxes react very sensitively to horizontal changes of the surface temperature. Fluxes calculated for longer length intervals represent a kind of average of fluxes over shorter length intervals. The quality of the aircraft-based fluxes is further manifested by the good agreement between them and fluxes measured at ice stations during BASIS (heat flux difference is typically within a few Wm^{-2} [Brümmer *et al.*, 2002]).

[17] The random errors ($s_{Rw'x'}$) of the fluxes were quantified for all low-level flight legs according to *Kaimal and Finnigan* [1994] and the systematic errors ($s_{Sw'x'}$) according to *Lenschow et al.* [1994],

$$s_{Rw'x'} = \sqrt{\frac{2\sigma_{w'x'}^2 \Lambda_{w'x'}}{l}} \quad (13)$$

$$s_{Sw'x'} = \frac{2\Lambda_{w'x'} \overline{w'x'}}{l}, \quad (14)$$

where σ is the variance, Λ is the integral length scale determined as the 10% value of the autocorrelation function, and l is the sampling length.

[18] Applying sampling lengths of 1, 2, 4, 8, 12, 16, 20, and 30 km, the random and the systematic flux errors were studied as a function of the fluxes themselves. For example, the turbulent fluxes τ and H and their errors are shown for $l = 8$ km in Figures 3a and 3b. The mean relative error is defined as the ratio of the mean error and the mean flux. The dependence of the relative random and systematic errors on the sampling length is shown in Figures 3c and 3d. The relative random error of H decreases from 47% for $l = 1$ km to 22% for $l = 8$ km. It is striking that a further increase of l does not reduce the relative error any more. The relative random error of τ is larger and decreases from 85% for $l = 1$ km to 30% for $l = 20$ km. The systematic errors are generally smaller and even close to zero for sampling lengths of more than 8 km. As a conclusion, 8 km is regarded as a proper sampling length: On the one hand, it is long enough to capture the relevant turbulent motions and to warrant statistical significance. On the other hand, a larger l would raise difficulties regarding the linear detrending in cases of a strong mesoscale variability.

2.3. Selection of Measurement Cases

[19] The calculation of roughness lengths (from equations (7)–(9)) and neutral transfer coefficients (from equations (4) and (5) setting the universal functions $\psi(z/L) = 0$ and the reference height $z = 10$ m) requires accurate data. The accuracy increases with increasing magnitudes of V , $\Delta\Theta$, Δq , H , and E . To be on the safe side, we include only those measurement cases in our analyses where the magnitudes are at least 3 times larger than the measurement errors: $V > 1.5 \text{ m s}^{-1}$, $\Delta\Theta > 2.25 \text{ K}$, $H > 6 \text{ Wm}^{-2}$, and $\tau > 1.5 \times 10^{-2} \text{ Nm}^{-2}$.

[20] The transfer coefficients depend on the reference height z as shown in equations (4) and (5). Equations (1)–(9) are based on the assumption of a constant-flux

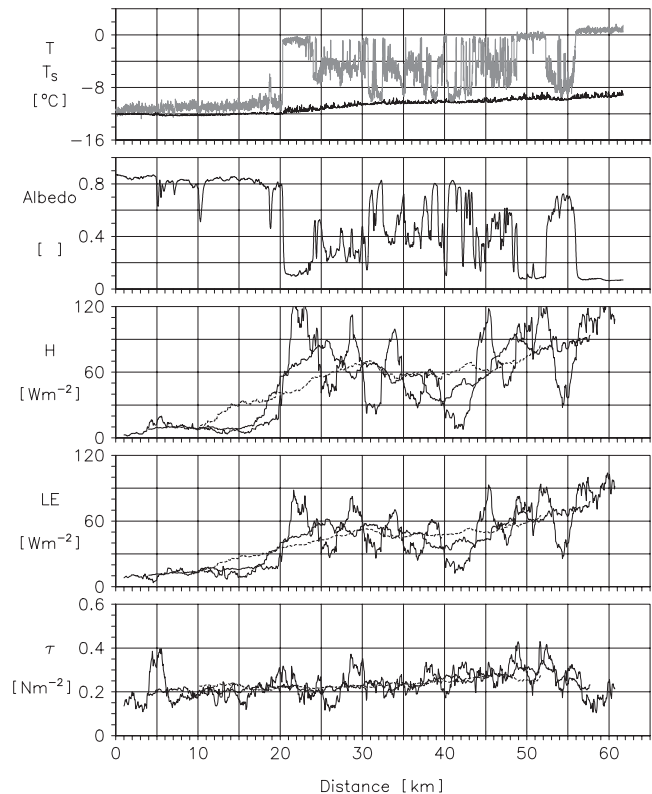


Figure 2. Air temperature T , surface temperature T_s (shading), albedo, sensible heat flux H , latent heat flux LE , and momentum flux τ measured at 30 m height on 5 March 1998 (leg 8). The fluxes are calculated for 2 (thin line), 8 (thick line), and 20 km (dashed line) length intervals and shifted by 50 m.

layer; that is, the fluxes are constant in height at least up to z . In a stable boundary layer the assumption of a constant-flux layer is questionable. On the basis of aircraft measurements in the Fram Strait, *Hartmann et al.* [1994] found that under stable stratification the flight level of about 40 m was decoupled from the surface processes. The vertical flux profile in the lowest 30 m was studied by *Forrer and Rotach* [1997] based on tower data over the Greenland ice sheet. The heat fluxes were not constant with height, even under slightly stable stratification. Although the Monin-Obukhov similarity theory is generally used in atmospheric models, its application is debatable under stable stratification [e.g., *Pahlow et al.*, 2001]. Our aircraft observations cover the whole stability range over broken sea ice, but to avoid the above mentioned problems, we restrict to unstable boundary layer cases only. In this way, 32 independent cases with $l = 8$ km, ice concentration $0.1 < n_{ice} < 1$, and heights $z < 35$ m were selected.

3. Ice Characteristics During the Selected Cases

[21] In order to characterize the various ice conditions under which the measurements were taken, Figure 4 shows air temperature, surface temperature, and surface albedo for the 8-km cases. Note that cases 1–21 are from the Baltic Sea and cases 22–32 are from the Fram Strait. Whereas the air temperature is nearly constant in horizontal direction in

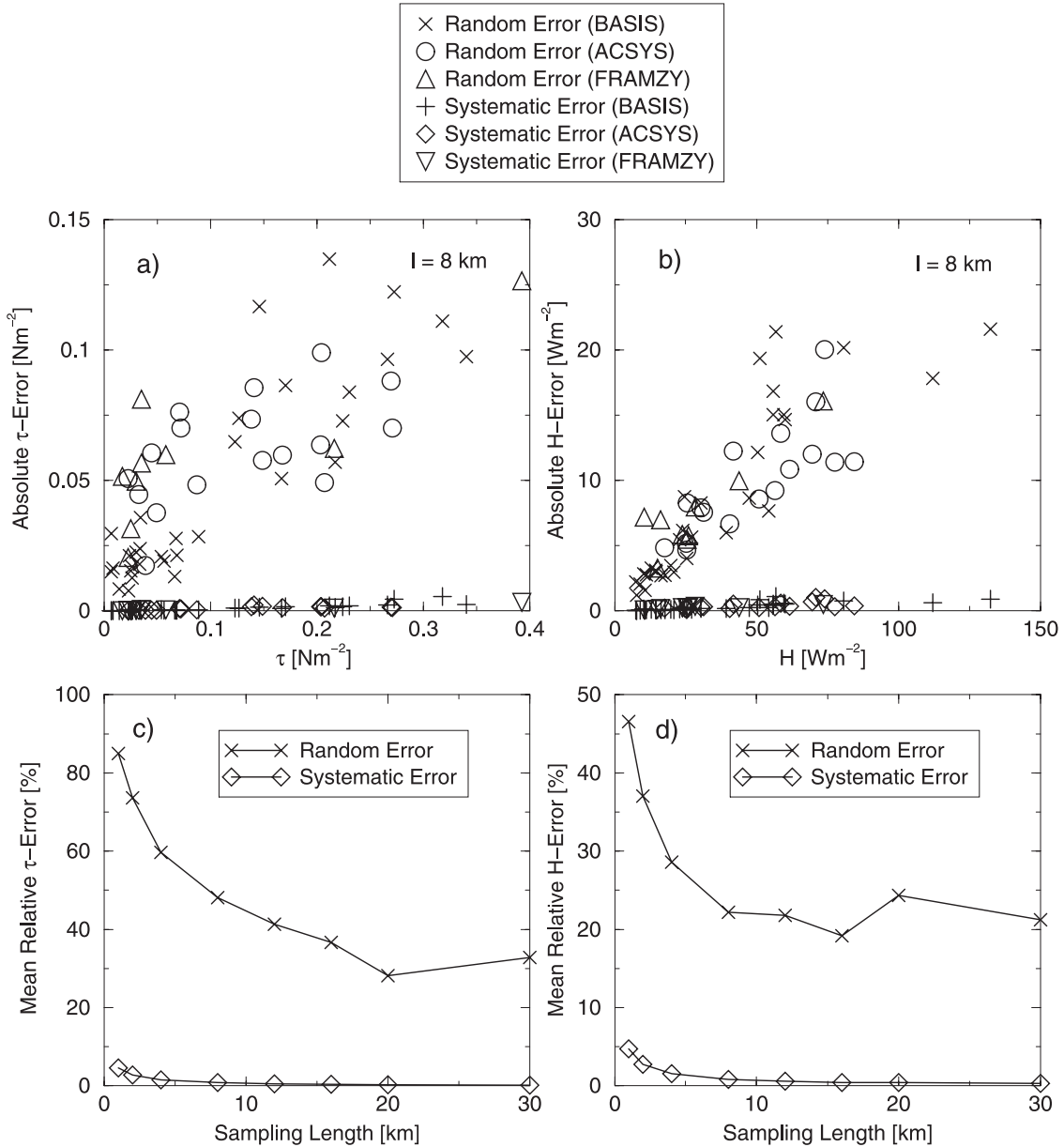


Figure 3. Random and systematic errors of the aircraft-based turbulent fluxes. Absolute errors versus magnitude of (a) momentum flux τ and (b) sensible heat flux H for sampling length $l = 8$ km. Relative errors versus sampling length for (c) τ and (d) H . The calculations are based on all horizontal flight legs at heights lower than 35 m under unstable stratification during BASIS, ACSYS, and FRAMZY.

each case, the surface temperature varies according to the differences between open water and various ice types. The albedo follows the horizontal variations of T_s in a smoothed way due to the 180° aperture angle of the pyranometers compared to the 2° aperture angle of the infrared surface temperature radiometer. For each case measurement height, ice concentration, ice surface albedo, air temperature, mean surface temperature, ice temperature, areal fraction of stable stratification ($\theta - \theta_s > 0$), wind speed, and visual ice observations are listed in Table 1. The 32 cases can be classified into the following six ice categories.

3.1. Gray Young Ice

[22] The Baltic Sea cases 1, 2, 3, 5, 6, and 20 evince a low albedo between 0.1 and 0.4 and rather small variations

of surface temperature. Nilas, pancake ice, and frazil ice as shown by two photos (Figures 5a and 5b) belong to this category.

3.2. Mixture of Gray and White First-Year Ice and Leads

[23] The Baltic Sea cases 7, 8, 9, 10, 12, 13, 14, 17, 18, and 21 and the Fram Strait cases 23 and 31 show alternating white snow-covered and gray ice parts or leads. An example photography is given in Figure 5c. In all Baltic Sea cases the white level ice is relatively thin (< 0.5 m), the free-board is low (~ 0.06 m), and thus the geometric roughness is not particularly large. The differences between open water and ice surface temperature range between 5 K (case 12) and 20 K (case 23).

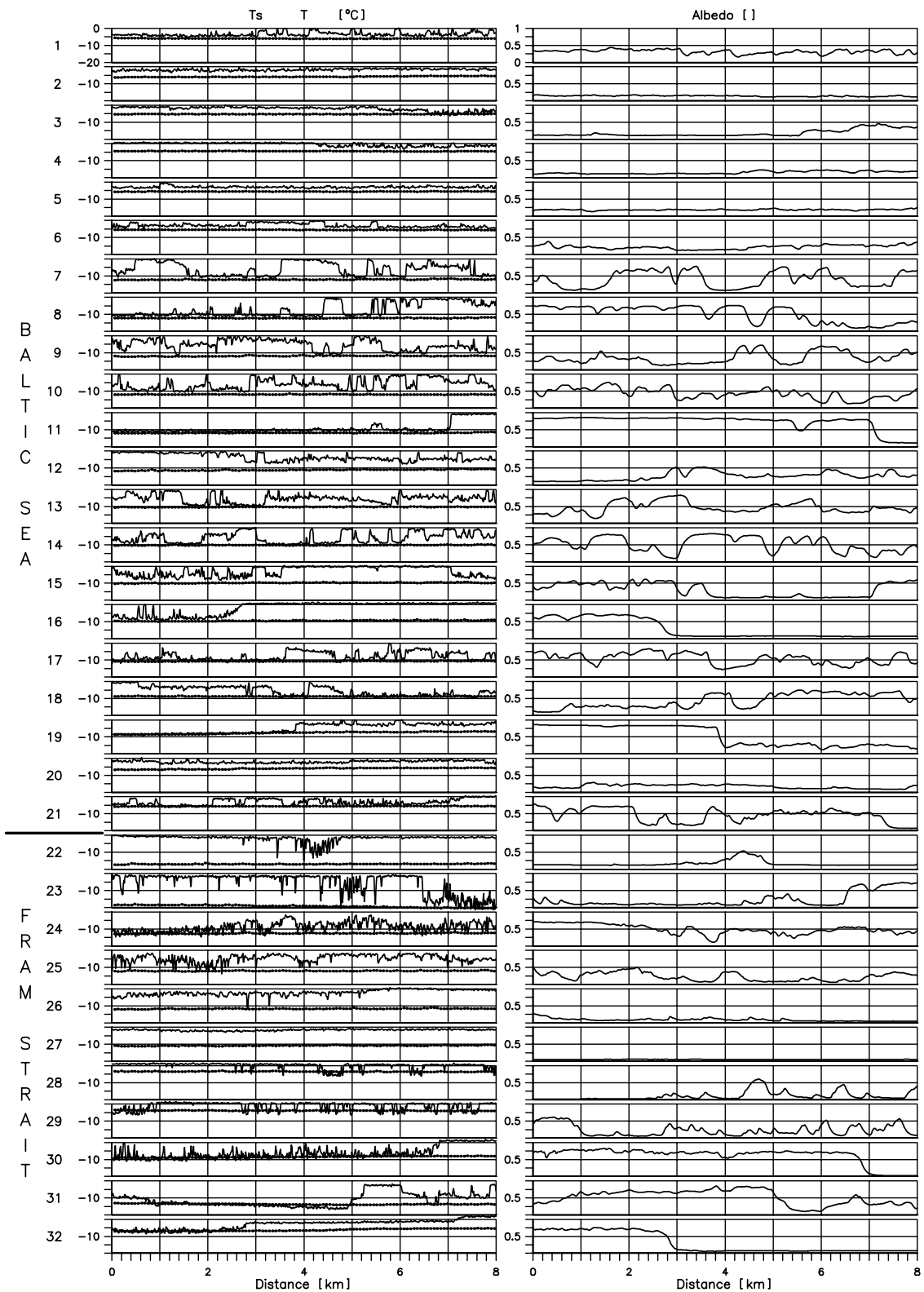


Figure 4. Air temperature T (dotted), surface temperature T_s , and albedo of 32 individual cases measured in the MIZ of the Baltic Sea (cases 1–21) and the Fram Strait (cases 22–32).

Table 1. Thirty-Two Individual Cases With a Horizontal Length of 8 km Measured in the MIZ of the Baltic Sea (Cases 1–21) and the Fram Strait (Cases 22–32)^a

Number	Day	h , m	n_{ice}	A_i	T_{as} , °C	T_{ss} , °C	T_{is} , °C	Stable Fraction	V , m s ⁻¹	Visual Ice Observations
1	03–02–1998	12	0.93	0.34	-5.9	-3.4	-3.6	0.00	3.4	gray ice, gobbets
2	03–02–1998	9	0.94	0.15	-5.8	-1.7	-1.7	0.00	3.2	gray, thin, smooth ice
3	03–02–1998	9	0.92	0.19	-5.2	-2.0	-2.2	0.04	3.3	gray and pancake ice
4	03–02–1998	17	0.35	0.30	-4.4	-0.4	-1.7	0.00	4.0	frazil ice
5	03–03–1998	15	0.99	0.19	-5.6	-2.9	-2.9	0.00	4.6	thin, gray, new ice
6	03–03–1998	15	0.93	0.23	-5.5	-2.8	-3.0	0.00	5.2	thin, gray, new ice
7	03–05–1998	17	0.84	0.47	-12.1	-5.9	-7.0	0.00	12.0	intermittent white and gray ice
8	03–05–1998	34	0.94	0.54	-12.2	-7.2	-7.6	0.01	11.6	intermittent white and gray ice
9	03–05–1998	29	0.95	0.37	-11.9	-5.3	-5.6	0.00	11.9	intermittent white and gray ice
10	03–05–1998	31	0.91	0.47	-11.9	-5.8	-6.3	0.00	11.7	intermittent white and gray ice
11	03–05–1998	33	0.96	0.76	-11.9	-9.3	-9.7	0.01	10.3	white, solid ice, open ponds
12	03–05–1998	28	0.86	0.29	-11.1	-3.6	-4.0	0.00	10.4	open ponds, large ice fields
13	03–05–1998	28	0.96	0.48	-10.4	-5.4	-5.7	0.00	10.1	open ponds, large ice fields
14	03–05–1998	29	0.91	0.57	-10.2	-5.8	-6.3	0.02	9.9	open ponds, large ice fields
15	03–05–1998	26	0.54	0.50	-9.7	-2.9	-5.2	0.00	10.4	first ice edge
16	03–05–1998	33	0.33	0.68	-9.4	-1.8	-7.1	0.00	9.6	second ice edge
17	03–06–1998	17	0.99	0.55	-10.7	-7.8	-7.8	0.10	5.7	nilas
18	03–06–1998	15	0.95	0.45	-8.8	-5.5	-5.8	0.20	5.1	almost 100% ice
19	03–06–1998	18	0.96	0.54	-7.6	-5.0	-5.2	0.24	7.4	first white ice, later gray ice
20	03–06–1998	17	0.96	0.18	-6.0	-2.0	-2.1	0.00	7.4	gray ice
21	03–06–1998	15	0.87	0.51	-5.6	-3.1	-3.6	0.10	4.0	intermittent white and gray ice
22	03–20–1998	20	0.11	0.89	-17.0	-1.8	-6.4	0.00	2.5	loose ice fields
23	03–20–1998	17	0.37	0.50	-19.2	-5.3	-11.6	0.02	4.3	diffuse ice edge, pancake ice
24	03–20–1998	16	0.99	0.50	-12.5	-8.7	-8.8	0.11	4.6	a wide ice edge zone
25	03–20–1998	13	0.84	0.26	-12.0	-4.7	-5.2	0.01	4.5	a wide ice edge zone
26	03–20–1998	16	0.43	0.11	-11.7	-2.1	-3.6	0.00	4.3	a wide ice edge zone
27	03–20–1998	15	0.11	0.07	-10.8	-1.6	-2.5	0.00	4.5	grease ice
28	03–21–1998	19	0.12	0.42	-3.5	0.1	-4.6	0.10	10.8	loose ice fields
29	03–21–1998	20	0.26	0.71	-3.8	-1.0	-4.7	0.20	9.9	loose ice fields
30	04–10–1999	15	0.81	0.75	-8.4	-6.0	-7.6	0.32	12.0	ice edge
31	04–12–1999	16	0.97	0.54	-13.6	-11.2	-11.4	0.46	11.8	broken ice, ponds covered by ice
32	04–14–1999	16	0.39	0.65	-6.3	-3.1	-6.1	0.17	4.6	ice edge

^aMeasurement height h , ice concentration n_{ice} , ice surface albedo A_i , air, mean surface, and ice temperature, T_{as} , T_{ss} , and T_{is} , fraction of stable boundary layer, wind speed V , and visual ice observations. Ice surface albedo A_i is determined by $A_i = [A - A_w \times (1 - n_{ice})]/n_{ice}$ with water surface albedo $A_w = 0.07$ and measured mean albedo A .

3.3. Rough Multi-Year Ice

[24] The Fram Strait cases 24 and 25 are striking because of a high-frequency variability of surface temperature caused by alteration of small but thick rough ice floes and leads.

3.4. Step Change Between Ice and Open Water

[25] All cases showing a prominent step between ice and open water (cases 4, 11, 15, 16, 19, 26, 30, and 32) are included into this category. A photo of the ice edge of the Baltic Sea on 5 March 1998 (case 16) is presented in Figure 5d. There are cases with moderate differences between ice and water temperature (10 K in case 11) and cases with small differences (1.5 K in case 4).

3.5. Loose Ice Fields

[26] During cases 22, 28, and 29 loose ice fields were passed over as shown in Figure 5f. Whereas the air temperature ($T = -17^\circ\text{C}$) is clearly colder than the ice surface temperature ($T_s = -6^\circ\text{C}$) under low wind conditions in case 22, air and ice temperature are both around -4°C with a wind speed around 10 m s^{-1} in cases 28 and 29.

3.6. Grease Ice

[27] Furthermore, one case of grease ice with a very low ice surface albedo of 0.07 (case 27, see Figure 5e) is included in our study.

4. Roughness Lengths and Neutral Transfer Coefficients

4.1. Mean Values for Experimental Regions and Sea Ice Categories

[28] The roughness lengths, the neutral transfer coefficients, the ice concentration, the surface albedo, the vertical potential temperature difference, and the wind speed are listed in Table 2 averaged for the two experimental areas and the six ice categories. The means of the roughness lengths are calculated as logarithmic means. For the Baltic Sea, the mean z_0 -value of $3 \times 10^{-4} \text{ m}$ is close to the results of *Launiainen et al.* [2001] obtained for land-fast ice during the same experiment using ice-based tower measurements. The roughness lengths z_T and z_q amount to $2 \times 10^{-8} \text{ m}$ and $4 \times 10^{-7} \text{ m}$ being 3 to 4 orders of magnitude smaller than z_0 . In the Fram Strait we obtain $z_0 = 2 \times 10^{-3} \text{ m}$, $z_T = 3 \times 10^{-9} \text{ m}$, and $z_q = 1 \times 10^{-8} \text{ m}$. Averaging over all 32 cases, the mean roughness lengths are $z_0 = 5 \times 10^{-4} \text{ m}$, $z_T = 1 \times 10^{-8} \text{ m}$, and $z_q = 1 \times 10^{-7} \text{ m}$. This corresponds to neutral transfer coefficients referred to 10 m of $C_{DN10} = (1.9 \pm 0.8) \times 10^{-3}$, $C_{HN10} = (0.9 \pm 0.3) \times 10^{-3}$, and $C_{EN10} = (1.0 \pm 0.2) \times 10^{-3}$. The standard deviations are calculated as the root mean square errors of the 32 cases.

[29] Studying the six ice categories, clear differences between the C_{DN10} -values are identifiable and to a certain extent explainable. The ice categories “gray young ice” and “mixture of gray and white first-year ice and leads”

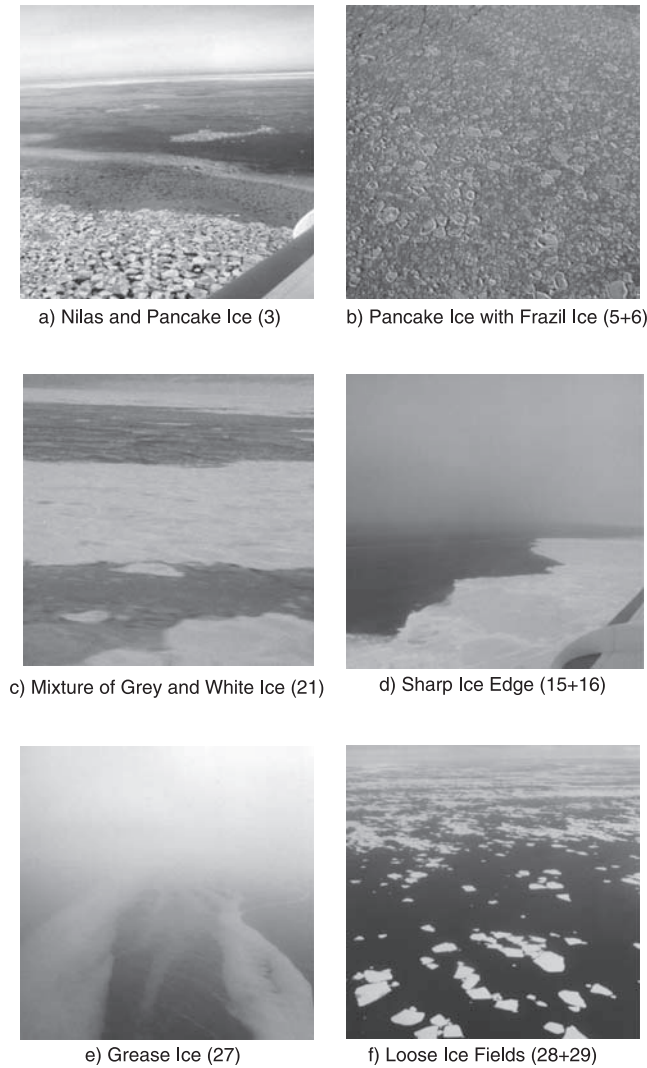


Figure 5. Six photos representing different ice characteristics in the MIZ of the Baltic Sea and the Fram Strait. The numbers in brackets refer to the cases given in Table 1. The photos were taken at flight heights of less than 100 m.

represent thin and smooth ice leading to a C_{DN10} of 1.5×10^{-3} . Over a step change between ice and open water and over loose ice fields the roughness is enlarged ($C_{DN10} = 2.0 \times 10^{-3}$ and 2.2×10^{-3} , respectively), and many thick and rough ice floes lead to the very large C_{DN10} of 4.5×10^{-3} for the category “rough multi-year ice.” The large C_{DN10} value of 2.5×10^{-3} for the grease ice is surprising. Altogether, there is a wide range of momentum roughness lengths in the MIZ. In contrast to the momentum exchange, C_{HN10} and C_{EN10} are always around 1.0×10^{-3} , except for the category of the rough ice ($C_{HN10} = 1.5 \times 10^{-3}$ and $C_{EN10} = 1.3 \times 10^{-3}$). The coefficients for the heat exchange obviously depend less strongly on the ice characteristics than that for the momentum exchange, and they are clearly smaller at all six categories.

[30] The above mentioned findings do not depend on the sampling length. The mean results for $l = 2$ km and $l = 20$ km, based on 103 and 10 cases, respectively, are listed in Table 2 and do not differ essentially from those for $l = 8$ km.

Table 2. Effective Roughness Lengths for Momentum z_0 , Sensible Heat z_q and Latent Heat z_l and Neutral Transfer Coefficient C_{DN10} , C_{HN10} , and C_{EN10} Determined From Aircraft Flights Over the Baltic Sea (BASIS 1998) and the Fram Strait (ACSYS 1998 and FRAMZY 1999)^a

	Number of Cases	n_{ice}	A_i	V_i , $m\ s^{-1}$	$\Delta\Theta$, K	z_0 , m	z_l , m	z_q , m	$C_{DN10} \times 10^3$	$C_{HN10} \times 10^3$	$C_{EN10} \times 10^3$
Baltic Sea	21	0.86	0.41	7.7	4.4	3×10^{-4}	2×10^{-8}	4×10^{-7}	1.6 ± 0.5	0.9 ± 0.2	1.0 ± 0.2
Fram Strait	11	0.49	0.48	6.7	6.7	2×10^{-3}	3×10^{-9}	1×10^{-8}	2.5 ± 1.0	1.0 ± 0.3	1.0 ± 0.3
Total (MIZ)	32	0.73	0.43	7.3	5.2	5×10^{-4}	1×10^{-8}	1×10^{-7}	1.9 ± 0.8	0.9 ± 0.3	1.0 ± 0.2
Gray young ice	6 (1, 2, 3, 5, 6, 20)	0.94	0.21	4.5	3.2	2×10^{-4}	1×10^{-7}	2×10^{-7}	1.5 ± 0.3	0.9 ± 0.1	0.9 ± 0.2
Mixture of gray and white ice and leads	12 (7, 8, 9, 10, 12, 13, 14, 17, 18, 21, 23, 31)	0.88	0.47	9.0	5.5	2×10^{-4}	3×10^{-9}	2×10^{-7}	1.5 ± 0.5	0.8 ± 0.2	0.9 ± 0.3
Rough multi-year ice	2 (24, 25)	0.92	0.40	4.6	5.6	2×10^{-2}	8×10^{-8}	2×10^{-8}	4.5	1.5	1.3
Step change betw. ice and water	8 (4, 11, 15, 16, 19, 26, 30, 32)	0.60	0.57	7.8	4.8	9×10^{-4}	3×10^{-9}	9×10^{-8}	2.0 ± 0.4	0.9 ± 0.2	1.0 ± 0.2
Loose ice fields	3 (22, 28, 29)	0.16	0.70	7.7	7.2	2×10^{-3}	6×10^{-8}	5×10^{-8}	2.2 ± 0.2	1.0 ± 0.2	1.0 ± 0.2
Grease ice	1 (27)	0.11	0.07	4.5	9.2	3×10^{-3}	1×10^{-7}	3×10^{-7}	2.5	1.1	1.2
Total (2 km)	103	0.77	0.41	7.5	5.3	5×10^{-4}	1×10^{-10}	2×10^{-9}	2.0 ± 1.0	0.8 ± 0.4	0.9 ± 0.4
Total (20 km)	10	0.72	0.60	7.9	3.9	7×10^{-4}	7×10^{-9}	2×10^{-7}	1.9 ± 0.8	0.9 ± 0.2	1.0 ± 0.2
Open water	11	0.00	0.07 (A_w)	6.0	6.5	7×10^{-4}	5×10^{-8}	1×10^{-7}	1.9 ± 0.6	1.0 ± 0.2	1.0 ± 0.2

^aThe results hold for 8 km length intervals on principle and unstable stratification. The mean values of ice concentration n_{ice} , ice surface albedo A_i , wind speed V_i , and vertical potential temperature difference $\Delta\Theta$ are shown. For the six ice categories the numbers of the belonging cases are given in the second column (compare Table 1). In the last three rows all data are shown for length intervals of 2 and 20 km and for open water legs in the MIZ.

[31] The results for open water in the vicinity of ice edge in the last row of Table 2 are interesting in the sense that they do not differ from the average results over broken sea ice. In general, C_{DN} is larger over sea ice than over open sea [Guest and Davidson, 1991], but the reverse case has also been observed [Andreas et al., 1979]. Our C_{DN10} of 1.9×10^{-3} for the open water is close to that of Guest and Davidson [1991] for ice-free Arctic within 100 km of sea ice regions, but large compared to such well-known studies as those of Garratt [1977] and Smith [1988]. They are, however, based on measurements over mature wind waves far from the coast, and our data are from the vicinity of the ice edge, where the waves are still in their growing phase. A C_{DN10} of 1.9×10^{-3} for $V = 6.0 \text{ m s}^{-1}$ is at the upper limit of the range observed by Drennan et al. [1999] for such conditions.

4.2. Individual Cases

[32] Looking at the 32 cases individually (Figure 6), z_0 varies from 10^{-6} to 10^{-2} m and z_T from 10^{-16} to 10^{-4} m. The very small z_T values do not mean that the heat exchange between surface and air is practically prevented. This is because C_H depends on both roughness lengths z_0 and z_T (see equation (4)). For most of the 32 cases the ratios C_{HN}/C_{DN} and z_T/z_0 are smaller than those based on the work of Andreas [1987] shown for comparison in Figures 6a and 6b. The two outliers on the upper region, cases 24 and 25, represent very rough and small ice floes (see Figure 4). For such conditions the formulas of Andreas [1987] fit. In the lower region, case 10 measured during an off-ice air flow in the Baltic Sea on 5 March 1998 is striking. In spite of the large wind speed of 12 m s^{-1} and surface-air temperature difference of 6 K, the fluxes $\tau = 0.13 \text{ Nm}^{-2}$ and $H = 24 \text{ Wm}^{-2}$ are relatively small leading to very small roughness lengths. This flight leg was conducted along the wind direction. It may be that turbulence structures were not completely gathered. In a case of organized convection, the turbulent fluxes measured during a leg perpendicular to the air flow are larger than those measured during a leg parallel to the air flow [Brümmer, 1999]. This aspect is only mentioned here as a possible influencing factor, but has not been looked after systematically for all 32 cases.

[33] Small z_T -values were also determined for the cases 11, 30, and 32. Each of them contains a step change between ice and open water with z_0 -values larger than 10^{-3} , but, contrary to the momentum exchange, the heat exchange is not increased by the step change, leading to small z_T -values. The variety of the characteristics of sea ice cover in the 32 cases (ice thickness, size of ice floes, areal composition of ice floes, etc.) may explain that a simple dependence of C_{DN} on ice concentration, as shown, for example, by Mai et al. [1996], could not be found. The same holds for C_{HN} and the ratio C_{HN}/C_{DN} . In fact, ice concentration alone is not a sufficient property to characterize the sea ice roughness.

4.3. Sensitivity of the Derived Transfer Coefficients to Measurement Errors

[34] The calculated transfer coefficients depend on the accuracy of the measured data. It is known that the determination of C_{HN} is particularly sensitive to surface temperature measurement errors [e.g., Calanca, 2001]. To quantify the accuracy of our above results, the impact of

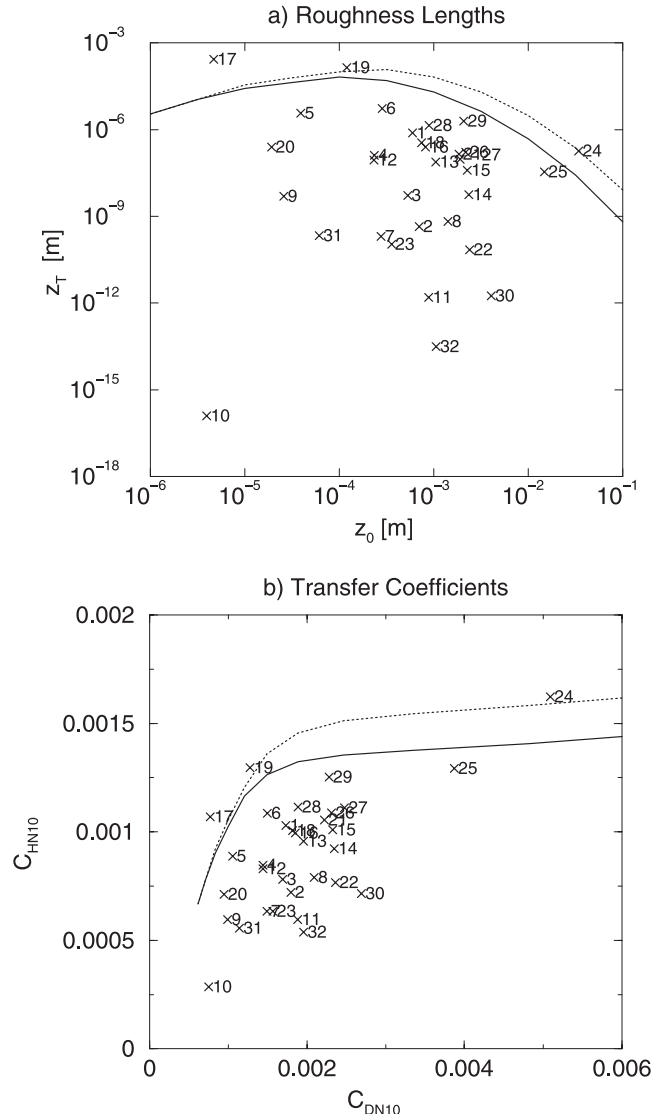


Figure 6. (a) The relation between the effective roughness lengths of momentum z_0 and heat z_T as well as (b) the neutral transfer coefficients reduced to 10 m of momentum C_{DN10} and heat C_{HN10} in the MIZ of the Baltic Sea and the Fram Strait. The numbers refer to cases listed in Table 1. For comparison, the relation based on work of Andreas [1987] is shown for $V = 5 \text{ m s}^{-1}$ (dotted line) and $V = 10 \text{ m s}^{-1}$ (solid line).

measurement errors of both the fluxes τ and H and the mean values $\Delta\Theta$ and V on the transfer coefficients C_{DN10} and C_{HN10} and their ratio is studied. The assumed error values and their impact are listed in Table 3.

[35] Considering the air-surface temperature difference, the systematic error $s_{\Delta\Theta}$ is set to 0.75 K. This is based on the assumption that the assumed total errors of surface and air temperature of 1 K and 0.5 K consist of a systematic and a random part of equal size. Increasing $\Delta\Theta$ by +0.75 K in all cases would decrease the mean C_{HN10} from 0.90 to 0.75×10^{-3} , whereas decreasing $\Delta\Theta$ by -0.75 K would lead to a mean C_{HN} value of 1.15×10^{-3} . Considering the wind speed, the systematic error s_V is assumed to be 0.5 m s^{-1}

Table 3. Sensitivity of the Neutral Transfer Coefficients for Momentum C_{DN10} and Sensible Heat C_{HN10} to Systematic Measurement Errors Concerning Vertical Potential Temperature Difference $\Delta\Theta$, Wind Speed V , Sensible Heat Flux H , and Momentum Flux τ

	$C_{DN10} \times 10^3$	$C_{HN10} \times 10^3$	C_{HN10}/C_{DN10}
Reference	1.89	0.90	0.47
$\Delta\Theta = \Delta\Theta + 0.75$ K	1.87	0.75	0.40
$\Delta\Theta = \Delta\Theta - 0.75$ K	1.93	1.15	0.60
$V = V + 0.5$ m s ⁻¹	1.65	0.84	0.51
$V = V - 0.5$ m s ⁻¹	2.21	0.96	0.44
$H = H + 1$ Wm ⁻²	1.89	0.96	0.51
+ (22% $\times H/\sqrt{32}$)			
$H = H - 1$ Wm ⁻²	1.89	0.84	0.44
- (22% $\times H/\sqrt{32}$)			
$\tau = \tau + 5 \times 10^{-3}$ Nm ⁻²	2.16	0.90	0.42
+ (48% $\times \tau/\sqrt{32}$)			
$\tau = \tau - 5 \times 10^{-3}$ Nm ⁻²	1.63	0.90	0.55
- (48% $\times \tau/\sqrt{32}$)			
$\Delta\Theta = \Delta\Theta -$, $V = V +$,	1.44	1.15	0.80
$H = H +$, $\tau = \tau -$			

based on a comparison between aircraft-based and surface-based wind data during BASIS 1998. A change of V by 0.5 m s⁻¹ modifies C_{DN10} by about $\pm 0.3 \times 10^{-3}$ and C_{HN} by $\pm 0.06 \times 10^{-3}$.

[36] For the fluxes, the systematic part of the error and the systematic impact of the random part of the error are regarded. The maximum calculated systematic errors of 1 Wm⁻² for H and 5×10^{-3} Nm⁻² for τ (equations (7) and (9); Figures 3a and 3b) and the mean relative errors of 22% for H and 48% for τ for $l = 8$ km (Figures 3c and 3d) are considered. The total errors taken into account are estimated as $s_H = 1$ Wm⁻² + $(0.22 \times H/\sqrt{N})$ and $s_\tau = 5 \times 10^{-3}$ Nm⁻² + $(0.48 \times \tau/\sqrt{N})$, where $N = 32$ represents the number of independent cases. The errors s_H and s_τ modify the ratio C_{HN10}/C_{DN10} by about 10%. A combination of all errors leading to the largest ratio of $C_{HN10}/C_{DN10} = 0.80$ is presented in the last row of Table 3. This ratio is close to that of *Andreas* [1987] for $C_{DN10} = 1.9 \times 10^{-3}$. For less rough ice ($C_{DN10} < 1.5 \times 10^{-3}$), even this upper limit of our ratio is smaller than the previous results of *Andreas* [1987] and *Launiainen et al.* [2001] over a compact ice cover.

[37] To what extent the ratio C_{HN10}/C_{DN10} is modified by a combined variation of V and $\Delta\Theta$ is revealed by Figure 7. We denote the variation in V and $\Delta\Theta$ by δV and $\delta(\Delta\Theta)$. The largest ratio of 0.77 occurs for $\delta V = +1$ m s⁻¹ and $\delta(\Delta\Theta) = -1$ K, and the smallest ratio of 0.32 for $\delta V = -1$ m s⁻¹ and $\delta(\Delta\Theta) = +1$ K. Figure 7 shows that the measurement accuracy has a distinct impact on the calculated roughness lengths and transfer coefficients over sea ice. However, even if the systematic measurement error had been somewhat larger than the 0.75 K and 0.5 m s⁻¹, our conclusion holds that the ratio C_{HN}/C_{DN} is much smaller than one.

5. Impact of the New Roughness Length for Heat on Parameterized Heat Flux

[38] The mean roughness length for heat of our study, $z_T = 1 \times 10^{-8}$ m, is significantly lower than the values generally used in atmospheric and sea ice models. To demonstrate the consequences of the new z_T on the parameterized fluxes, we compared the observed fluxes to those

based on three different assumption for z_T : (1) $z_T = z_0$, (2) $z_T = f(z_0, Re)$ according to *Andreas* [1987], and (3) $z_T = 1 \times 10^{-8}$ m. In all three cases z_0 is set to our mean value of 5×10^{-4} m and the universal functions of *Högström* [1988] are applied. The results are given in Figure 8. In the first case (Figure 8a), the mean parameterized H of 90 Wm⁻² is 49 Wm⁻² larger than the mean observed one. H is overestimated in all cases and the root-mean-square error (RMSE) amounts to 62 Wm⁻². The first case is included here because the assumption $z_T = z_0$ is usually made in weather and in climate models (e.g., the ECMWF model [*Deutsches Klimarechenzentrum*, 1994] and HIRLAM [*Källén*, 1996]). In the second case (Figure 8b), the discrepancies between measured and parameterized H are reduced, but H is still overestimated ($\Delta H = 32$ Wm⁻², RMSE = 41 Wm⁻²). In the third case (Figure 8c), the agreement is much better ($\Delta H = -3$ Wm⁻², RMSE = 15 Wm⁻²), but cannot be interpreted as a verification of our new roughness lengths and transfer coefficients because the same data set was used in deriving them. It is, however, noteworthy that simply applying a new constant z_T (that is not equal to z_0) reduces the RMSE-value by a factor of 3 to 4 in a data set that includes observations over various types of sea ice cover. Our z_T -modification leads to a relative reduction of H by a factor of more than 2 (on the average) and to an absolute reduction of up to 150 Wm⁻² in individual cases in comparison to the first case and up to 100 Wm⁻² in comparison to the second case, demonstrating the large sensitivity. Changes of such an order of magnitude have an important impact on the surface energy balance. It should be noted that we do not criticize the validity of *Andreas* [1987] over a compact ice cover (it was recently verified by *Andreas* [2002]), but show that the situation is different over a heterogeneous ice cover.

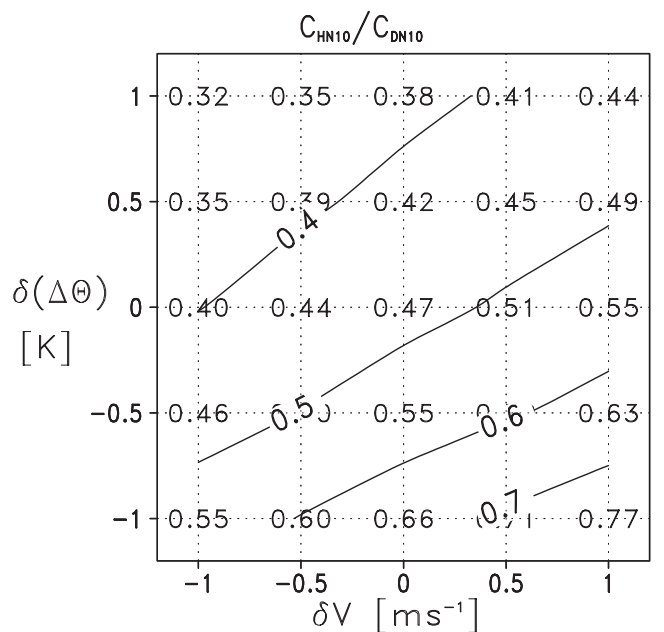


Figure 7. Dependence of the ratio of the transfer coefficients of heat and momentum C_{HN10}/C_{DN10} on systematic variations of the vertical difference of potential temperature $\delta(\Delta\Theta)$ and of wind speed δV .

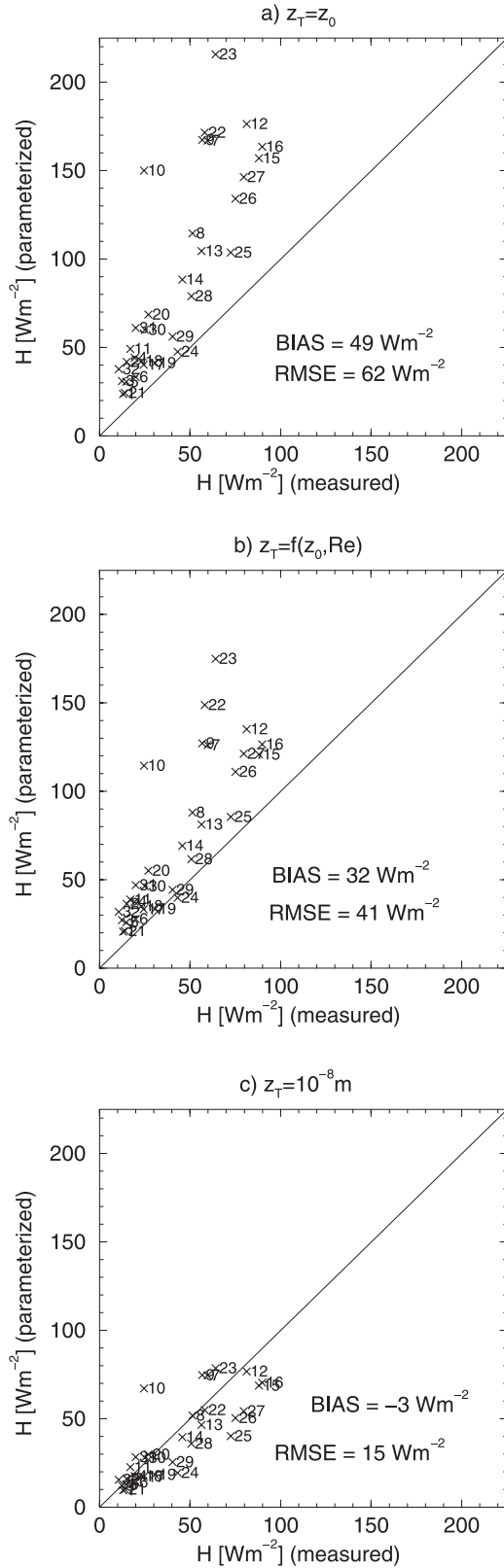


Figure 8. Measured versus parameterized sensible heat flux H based on 8 km samples and the universal functions of Högström [1988]: z_0 is set to our mean value of 5×10^{-4} m and z_T is set (a) equal to z_0 , (b) according to Andreas [1987], and (c) to our mean value of 10^{-8} m. The numbers refer to the cases listed in Table 1.

6. Concluding Remarks

[39] Turbulent heat and momentum fluxes as well as the surface temperature, air temperature, air humidity, and wind speed were measured by aircraft over the MIZ of the northern Baltic Sea and the Fram Strait. From these measurements, effective roughness lengths and corresponding transfer coefficients for momentum and sensible and latent heat were calculated. Aircraft-based fluxes sampled over 8-km intervals are proper for this purpose as manifested (1) by error calculations based on the methods suggested by Kaimal and Finnigan [1994] and Lenschow *et al.* [1994], (2) by the agreement between aircraft-based and surface-based fluxes observed during BASIS [Brümmer *et al.*, 2002], and (3) by the fact that the fluxes are very sensitive to independently measured variations of the underlying surface. We restricted our studies to unstable boundary layer cases, because under such conditions the aircraft-based surface flux estimates are less sensitive to measurement height. When calculating z_0 , z_T , and z_q , not only the fluxes but also the mean quantities (V , $\Delta\Theta$, Δq) have to be correct within acceptable limits. It is known that particularly the surface temperature is a sensitive parameter [e.g., Calanca, 2001]. To reduce the impact of measurement errors, we selected only cases in which the magnitudes of wind speed, temperature difference, and turbulent fluxes are at least three times larger than the measurement errors.

[40] The results show that the mean effective roughness lengths for sensible and latent heat ($z_T = 1 \times 10^{-8}$ m and $z_q = 1 \times 10^{-7}$ m) are 4 to 3 orders of magnitude smaller than those for momentum ($z_0 = 5 \times 10^{-4}$ m). The corresponding neutral transfer coefficients are $C_{DN10} = (1.9 \pm 0.8) \times 10^{-3}$, $C_{HN10} = (0.9 \pm 0.3) \times 10^{-3}$, and $C_{EN10} = (1.0 \pm 0.2) \times 10^{-3}$. Considering the ratios of the roughness lengths and transfer coefficients, our results obtained from measurements over the marginal sea ice zone differ from previously published results for compact sea ice [Andreas, 1987; Launiainen *et al.*, 2001]. This holds particularly for the less rough ice ($z_0 < 10^{-3}$ m), where our ratio of $z_0/z_T \approx 10^4$ is 2–5 orders of magnitude larger. For the very rough ice ($z_0 > 10^{-3}$ m) the differences are smaller and within the limits of inaccuracy of our results. We are not aware of previous observations of roughness lengths for heat over the MIZ. The ratio ($z_0/z_T \approx 10^4$) is, however, in agreement with observational results of Beljaars and Holtslag [1991] and Mahrt and Ek [1993] obtained for heterogeneous land surfaces. This appears to be reasonable, because from the point of view of the surface temperature distribution, a mixture of sea ice and leads resembles more a heterogeneous land surface than a compact ice cover.

[41] The question arises why z_T is so much smaller than z_0 over heterogeneous surfaces. A qualitative explanation is given by Beljaars and Holtslag [1991]: Sparsely distributed large obstacles increase the shear stress with height in the near-surface layer and therefore the effective z_0 is larger than the local z_0 of the prevalent surface cover. In contrast to momentum transfer, heat and moisture fluxes mainly depend on the net energy available at the surface. Thus the effective z_T has to be smaller than the local z_T and clearly smaller than the effective z_0 [see Beljaars and Holtslag, 1991, Figure 6]. Transferred to a broken sea ice cover, z_T is relatively small due to larger areas of flat ice, whereas z_0 is increased by the ice ridges and floe edges. Further, the form

drag caused by ridges and floe edges does not directly affect heat exchange and C_{HN10} , which depend both on z_0 and z_T . Hence, to compensate for the effect of increased z_0 in C_{HN10} , z_T must be decreased. Therefore z_T over a broken sea ice is lower than that over uniform sea ice. In the presence of ice ridges (larger z_0), z_T decreases also in the work by *Andreas* [1987], but in our case the decrease is larger. This may be related to the fact that we study a heterogeneous surface, over which the validity of Monin-Obukhov similarity theory is not guaranteed. In lieu of any better theory, weather prediction and climate models apply Monin-Obukhov similarity theory over various kinds of Earth's heterogeneous surface. This is relevant because, also, over heterogeneous surface the turbulent surface fluxes (τ , H , and LE) depend on the surface-air differences of the mean quantities (V , Θ , and q). The quantitative dependence and the structure of turbulence may, however, be different from that over a homogeneous surface. Accordingly, experimentally based parameter values are needed to describe the flux-profile relationships over heterogeneous surfaces, and it is reasonable that these parameter values may differ from those found for homogeneous surfaces.

[42] The observed sea ice in the MIZ shows a high degree of variability concerning floe size and horizontal distribution, ice thickness, and free-board height. Thus a wide range of z_0 -values from 10^{-6} to 10^{-2} m occurred. This explains why a simple dependence of C_{DN10} on only one parameter, namely ice concentration, could not be found.

[43] A comparison between the measured and parameterized fluxes using different roughness lengths shows that (1) the commonly used parameterizations ($z_T = z_0$) strongly overestimate the surface heat fluxes over a broken sea ice cover and (2) realistic heat fluxes can be parameterized if significantly smaller values for z_T than for z_0 are used.

[44] **Acknowledgments.** We particularly acknowledge the fruitful discussions with Jouko Launiainen from the Finnish Institute of Marine Research, Helsinki. The study was supported by the European Commission under the contract MAST3-CT97-0117 (BALTEX-BASIS), by the Deutsche Forschungsgemeinschaft under SFB-512 (FRAMZY), and by the Bundesministerium für Bildung und Forschung under 03PL020H (ACSYS).

References

- Andreas, E. L., A theory for the scalar roughness and the scalar transfer coefficients over snow and sea ice, *Boundary Layer Meteorol.*, **38**, 159–184, 1987.
- Andreas, E. L., Parameterizing scalar transfer over snow and ice: A review, *J. Hydrometeorol.*, **3**, 417–432, 2002.
- Andreas, E. L., C. A. Paulson, R. M. Williams, R. W. Lindsay, and J. A. Businger, The turbulent heat flux from Arctic leads, *Boundary Layer Meteorol.*, **17**, 57–91, 1979.
- Banke, E. G., S. D. Smith, and R. J. Anderson, Drag coefficients at AIDJEX from sonic anemometer measurements, in *Sea ice processes and models, Proceedings of the AIDJEX/ICSI Symposium, Seattle*, edited by R. S. Pritchard, pp. 430–442, Univ. of Washington Press, Seattle, 1980.
- Beljaars, A. C. M., The parameterization of surface fluxes in large-scale models under free convection, *Q. J. R. Meteorol. Soc.*, **121**, 255–270, 1994.
- Beljaars, A. C. M., and A. A. M. Holtslag, Flux parameterization over land surfaces for atmospheric models, *J. Appl. Meteorol.*, **30**, 327–341, 1991.
- Beljaars, A. C. M., and P. Viterbo, The sensitivity of winter evaporation to the formulation of aerodynamic resistance in the ECMWF model, *Boundary Layer Meteorol.*, **71**, 135–149, 1994.
- Brümmer, B., Roll and cell convection in wintertime Arctic cold-air outbreaks, *J. Atmos. Sci.*, **56**, 2613–2636, 1999.
- Brümmer, B., (Ed.), Field experiment FRAMZY 1999-Cyclones over the Fram Strait and their impact on sea ice, Field report with examples of measurements, *Ber. Zentrum Meeres Klimaforsch., Reihe A*, **33**, 2000.
- Brümmer, B., and S. Thiemann, Field Campaign ACSYS 1998: Aircraft measurements in Arctic on-ice air flows, *Ber. Zentrum Meeres Klimaforsch., Reihe A*, **32**, 1999.
- Brümmer, B., D. Schröder, J. Launiainen, T. Vihma, A. S. Smedman, and M. Magnusson, Temporal and spatial variability of surface fluxes over the ice edge zone in the northern Baltic Sea, *J. Geophys. Res.*, **107**(C8), 3096, doi:10.1029/2001JC000884, 2002.
- Calanca, P., A note on the roughness length for temperature over melting snow and ice, *Q. J. R. Meteorol. Soc.*, **127**, 255–260, 2001.
- Charnock, H., Wind stress on a water surface, *Q. J. R. Meteorol. Soc.*, **81**, 639–640, 1955.
- DeCosmo, J., K. B. Katsaros, S. D. Smith, R. J. Anderson, W. A. Oost, K. Bumke, and H. Chadwick, Air-sea exchange of water vapor and sensible heat: The Humidity Exchange Over the Sea (HEXOS) results, *J. Geophys. Res.*, **101**(C5), 12,001–12,016, 1996.
- Deutsches Klimarechenzentrum, The ECHAM 3 Atmospheric General Circulation Model, *Tech. Rep. 6*, Modellbetreuungsgruppe, Hamburg, Germany, 1994.
- Donelan, M. A., F. W. Dobson, S. D. Smith, and R. J. Anderson, On the dependence of sea surface roughness on wave development, *J. Phys. Oceanogr.*, **23**, 2143–2149, 1993.
- Drennan, W. M., K. K. Kahma, and M. A. Donelan, On momentum flux and velocity spectra over waves, *Boundary Layer Meteorol.*, **92**, 489–515, 1999.
- Forrer, J., and M. W. Rotach, On the turbulence structure in the stable boundary layer over the Greenland ice sheet, *Boundary Layer Meteorol.*, **85**, 111–136, 1997.
- Garratt, J. R., Review of drag coefficients over oceans and continents, *Mon. Weather Rev.*, **105**, 915–929, 1977.
- Garratt, J. R., Sensitivity of climate simulations to land-surface and atmospheric boundary-layer treatments—A review, *J. Clim.*, **3**, 419–449, 1993.
- Guest, P. S., and K. L. Davidson, The aerodynamic roughness of different types of sea ice, *J. of Geophys. Res.*, **96**(C3), 4709–4721, 1991.
- Hartmann, J., C. Kottmeier, C. Wamser, and E. Augstein, Aircraft measured atmospheric momentum, heat and radiation fluxes over Arctic sea ice, in *The Polar Oceans and Their Role in Shaping the Global Environment, Geophys. Monogr. Ser.*, vol. 85, edited by O. M. Johannessen et al., pp. 443–454, AGU, Washington, D. C., 1994.
- Högström, U., Non-dimensional wind and temperature profiles in the atmospheric surface layer: A re-evaluation, *Boundary Layer Meteorol.*, **42**, 55–78, 1988.
- Holtslag, A. A. M., and H. A. R. De Bruin, Applied modeling of the nighttime surface energy balance over land, *J. Appl. Meteorol.*, **27**, 689–704, 1988.
- Kaimal, J. C., and J. J. Finnigan, *Atmospheric Boundary Layer Flows*, pp. 254–280, Oxford Univ. Press, New York, 1994.
- Källen, E., (Ed.), HIRLAM Documentation Manual 2.5, Swedish Meteorol. and Hydrol. Inst., Stockholm, Sweden, 1996.
- Launiainen, J., (Ed.), BALTEX-BASIS Data Report 1998, *Publ. 14*, BALTEX Secretariat, Geesthacht, Germany, 1999.
- Launiainen, J., B. Cheng, J. Uotila, and T. Vihma, Turbulent surface fluxes and air-ice coupling in BALTEX-BASIS, *Ann. Glaciol.*, **33**, 237–242, 2001.
- Lenschow, D. H., J. Mann, and L. Kristensen, How long is long enough when measuring fluxes and other turbulence statistics?, *J. Atmos. Oceanic Technol.*, **11**, 661–673, 1994.
- Mahrt, L., and M. Ek, Spatial variability of turbulent fluxes and roughness lengths in HAPEX-MOBILHY, *Boundary Layer Meteorol.*, **65**, 381–400, 1993.
- Mai, S., C. Wamser, and C. Kottmeier, Geometric and aerodynamic roughness of sea ice, *Boundary Layer Meteorol.*, **77**, 233–248, 1996.
- Pahlow, M., M. B. Parlange, and F. Porte-Agel, On Monin-Obukhov similarity in the stable atmospheric boundary layer, *Boundary Layer Meteorol.*, **99**, 225–248, 2001.
- Smith, S. D., Coefficients for sea surface wind stress, heat flux, and wind profiles as a function for wind speed and temperature, *J. Geophys. Res.*, **93**(C12), 15,467–15,472, 1988.
- Uotila, J., Observed and modelled sea-ice drift response to wind forcing in the northern Baltic Sea, *Tellus, Ser. A*, **53**, 112–128, 2001.
- Wood, N., and P. Mason, The influence of static stability on the effective roughness lengths for momentum and heat transfer, *Q. J. R. Meteorol. Soc.*, **117**, 1025–1056, 1991.

B. Brümmer, A. Kerber, and D. Schröder, Meteorological Institute, University of Hamburg, Bundesstrasse 55, D-20146 Hamburg, Germany. (bruemmer@dkrz.de; kerber@dkrz.de; david.schroeder@dkrz.de)

T. Vihma, Finnish Institute of Marine Research, P.O. Box 33, FIN-00931 Helsinki, Finland. (Timo.Vihma@fimr.fi)